

Variational Wasserstein Barycenters with c -Cyclical Monotonicity

Jinjin Chi
Jilin University

Zhiyao Yang
Jilin University

Jihong Ouyang
Jilin University

Ximing Li
Jilin University

October 25, 2021

Abstract

Wasserstein barycenter, built on the theory of optimal transport, provides a powerful framework to aggregate probability distributions, and it has increasingly attracted great attention within the machine learning community. However, it suffers from severe computational burden, especially for high dimensional and continuous settings. To this end, we develop a novel continuous approximation method for the Wasserstein barycenters problem given sample access to the input distributions. The basic idea is to introduce a variational distribution as the approximation of the true continuous barycenter, so as to frame the barycenters computation problem as an optimization problem, where parameters of the variational distribution adjust the “proxy” distribution to be similar to the barycenter. Leveraging the variational distribution, we construct a tractable dual formulation for the regularized Wasserstein barycenter problem with c -cyclical monotonicity, which can be efficiently solved by stochastic optimization. We provide theoretical analysis on convergence and demonstrate the practical effectiveness of our method on real applications of subset posterior aggregation and synthetic data.

1 Introduction

Summarizing, combining and comparing probability distributions defined on a metric are fundamental tasks in machine learning, statistics and computer science, including multiple sensors, Bayesian inference, among others. For instance, in Bayesian inference one runs posterior sampling algorithm in parallel on different machines using small subsets of the massive data, and then aggregates subset posterior distributions via their *barycenter* as an approximation to the true posterior for the full data [1, 2]. Besides Bayesian inference, the average or barycenter of a collection of distributions has been successfully applied in various machine learning applications, say image processing [3] and clustering [4, 5].

The theory of *optimal transport* (OT) [6–9] provides a powerful framework to carry out such comparisons. OT equips the space of distributions with a distance metric known as the *Wasserstein distance*, which has gained substantial popularity in different fields, leading in particular to the natural consideration of barycenters. The *barycenter* of multiple given probability distributions under *Wasserstein distance* is defined as a distribution minimizing the sum of Wasserstein distances to all distributions. Due to the geometric properties of Wasserstein distance, the **Wasserstein barycenter** can better capture the underlying geometric structure than the barycenter with respect to other popular distances, e.g., Euclidean distance, see Figure 1. As a result, Wasserstein barycenters have a broad range of applications in text mixing [3], imaging [2, 10, 11], and model ensemble [12].

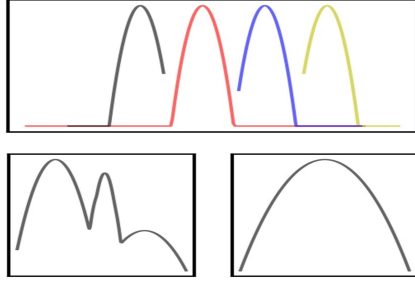


Figure 1: Top: four distributions. Bottom left: Euclidean average of distributions. Bottom right: Wasserstein barycenter.

Despite its impressive performance, the computation of the Wasserstein barycenter is challenging, especially for high dimensional and continuous settings [13]. Currently, the existing studies on computing the Wasserstein barycenter of continuous distributions require discretization of all input distributions or the barycenter itself, which scale poorly to high-dimensional settings. Moreover, the discretization technique of the continuous barycenter is undesirable since it lacks the inherently continuous nature of data distributions and ability of generating new samples when needed. To the best of our knowledge, very few techniques attempt to operate directly on continuous distributions and obtain a continuous barycenter. In this work, we further contribute on this challenging topic of continuous Wasserstein barycenter.

Our contributions As highlighted by [14], the *key challenge* of continuous Wasserstein barycenter problem is to find a suitable representation of the barycenter. Motivated by this, we introduce a family of continuous distributions, namely variational distributions, and find the closest one as the approximation of the true (continuous) barycenter. Thus, we frame barycenter computation problem as an optimization problem, where the parameters of variational distributions adjust the proxy distribution to be similar to the true barycenter. Following this, we propose a continuous computation method to approximate barycenters based on a novel regularized dual formulation, where we employ c -cyclical monotonicity regularization to obtain precise approximations. On the theoretical side, we prove the convergence of the proposed method. Finally, we demonstrate the practical effectiveness of our method, both on synthetic data and real applications on subset posterior aggregation.

Related work The notion of the Wasserstein barycenter was first introduced by [15] and then investigated by many works via the original Wasserstein distance as well as its regularization. Most of them mainly solve discrete Wasserstein barycenter problem, namely, averaging some discrete distributions, via linear programs (or some equivalent problem) [16–19] or regularized projection-based methods [4, 20–22].

However, these methods can not solve continuous Wasserstein barycenter problem, namely, averaging some continuous distributions. To address this issue, [23–25] assume the barycenter to be a finite points set and then operate the continuous input distributions. They compute the objective based on semi-discrete OT algorithms and use the discrete distribution as the approximation of the true barycenter.

The continuous approximation methods for Wasserstein barycenters of probability distributions over continuous spaces remain unexplored until recently [14, 26, 27]. Similar to our method, all

Literature	General cost	Barycenter	End-to-end
[14]	✓	Fixed prior	×
[26]	×	Generative network	×
[27]	×	Fixed prior	×
Our method	✓	Variational distribution	✓

Table 1: Summary of literature.

of them rely on dual formulation of the Wasserstein barycenter problem and represent the dual potentials with neural networks. However, these methods are not *end-to-end* (consist of two sequential steps), and recover barycenters via an additional estimation. The method in [14] computes dual potentials based on a regularized dual formulation via a stochastic algorithm and recovers the barycenter by pushing forward operator using gradients of potentials or by barycentric projection. Moreover, as highlighted by [14] this method assumes a fixed prior as the proxy of the barycenter from the beginning, which may be a poor proxy for the true barycenter resulting in the inaccurate approximations. Based on the specific ground cost, i.e., $c(x, y) = \frac{\|x-y\|^2}{2}$, [26, 27] compute the barycenters under Wasserstein-2 distance. The method in [26] employs the *generative network* to represent a barycenter and recovers it via a generative model or a pushforward map, which suffers from the usual limitations of generative networks such as mode collapse. Although this method does not involve the regularization terms, it ends up with a challenging min-max-min problem. The method in [27] constructs a regularized formulation by adding a congruence regularization to ensure that the optimal potential functions are consistent with the true barycenter, and then recovers the barycenter by using gradients of the potentials as pushforward maps. However, the congruence regularization requires selection of a prior distribution that is bounded below by the true barycenter, which is a non-trivial task. Besides, [28] proposes a generic algorithm to compute barycenters with respect to arbitrary discrepancies, which also parameterizes the barycenter by using a generative network. In contrast, our method is end-to-end and suitable for a general ground cost distance. Moreover, we consider c -cyclical monotonicity to make good approximations. Table 1 summarizes the existing studies on continuous Wasserstein barycenter calculation and shows our contribution.

2 Background and Preliminaries

In this section, we describe the Wasserstein barycenter problem, which involves all Wasserstein distances from one to many distributions.

Definition 1 (Wasserstein distance). *Let \mathcal{X} and \mathcal{Y} be arbitrary spaces equipped with a ground cost $c(x, y) = d(x, y)^p$. Given two continuous probability distributions $\mu(x)$ and $\nu(y)$, for $p \in [1, \infty)$, the Wasserstein distance between μ and ν is defined as follows [9]:*

$$W_p^p(\mu, \nu) = \inf_{\pi \in \Pi(\mu, \nu)} \int_{\mathcal{X}} \int_{\mathcal{Y}} \pi(x, y) c(x, y) dx dy, \quad (1)$$

where $\Pi(\mu, \nu)$ is the set of all joint distributions on $\mathcal{X} \times \mathcal{Y}$ with prescribed marginals $\mu(x)$ and $\nu(y)$. $d(\cdot, \cdot)$ is a distance on $\mathcal{X} \times \mathcal{Y}$.

The primal problem (1) admits an equivalent dual form [9]:

$$\sup_{\phi \oplus \psi \leq c} \int_{\mathcal{X}} \phi(x) \mu(x) dx + \int_{\mathcal{Y}} \psi(y) \nu(y) dy, \quad (2)$$

where ϕ and ψ are dual potentials, and $(\phi \oplus \psi)(x, y) \triangleq \phi(x) + \psi(y)$. The constraint $\phi \oplus \psi \leq c$ means $\phi(x) + \psi(y) \leq c(x, y)$ for all (x, y) .

Directly solving (1) and (2) is challenging, since the resulting linear program can be too costly. In order to speed up the computation, *regularized* OT was introduced by [29]. Here, we consider the entropy and L^2 -norm regularization:

$$\sup_{\phi, \psi} \int_{\mathcal{X} \times \mathcal{Y}} [\phi(x) \mu(x) + \psi(y) \nu(y) + F(\phi(x), \psi(y))] dx dy, \quad (3)$$

where

$$F(\phi(x), \psi(y)) = \begin{cases} -\varepsilon e^{\frac{1}{\varepsilon}(\phi(x) + \psi(y) - c(x, y))} & (\text{entropy}) \\ -\frac{1}{4\varepsilon}(\phi(x) + \psi(y) - c(x, y))_+^2 & (L^2) \end{cases} \quad (4)$$

Definition 2 (Wasserstein barycenter). *The Wasserstein barycenter of N ($N \geq 2$) continuous probability distributions μ_1, \dots, μ_N with weights $\alpha_1, \dots, \alpha_n \in \mathbb{R}_+$, is a solution of the following functional minimization problem [15]:*

$$\inf_{\nu} \sum_{i=1}^N \alpha_i W_p^p(\mu_i, \nu) \quad (5)$$

Regularized Wasserstein barycenter dual Since the primal objective (5) is hard to compute, we instead consider the dual formulation of regularized Wasserstein barycenter problem [14], which is a more popular and efficient alternative:

$$\inf_{\nu} \sup_{\substack{\phi, \psi \\ \sum_{i=1}^N \alpha_i \psi_i = 0}} \sum_{i=1}^N \alpha_i \left[\int_{\mathcal{X}} \phi_i(x_i) \mu_i(x_i) dx_i + \int_{\mathcal{X}} \int_{\mathcal{Y}} F(\phi_i(x_i) + \psi_i(y) - c(x_i, y)) \mu_i(x_i) \nu(y) dx_i dy \right] \quad (6)$$

where ϕ_i and ψ_i are dual potentials, and F refers to either entropy or L^2 -norm regularization. Note that ν is the true barycenter, not a prior like in [14].

Adding the regularization term makes the dual problem a concave maximization problem. We rely on this dual formulation in the next section to propose an efficient stochastic optimization algorithm.

3 Our Method

Our goal in this paper is to compute the Wasserstein barycenter for a given set of continuous distributions $\{\mu_1, \dots, \mu_N\}$. To effectively solve this problem, we present a novel end-to-end method with c -cyclical monotonicity, namely **Variational Wasserstein Barycenter (VWB)**, where the barycenter can be approximated by a variational distribution. Our method is well-suited for the case where the analytic forms of input distributions are not available. Since we only have access to independent samples which can be drawn from input distributions or are provided by machine learning applications.

3.1 Imposing the c -Cyclical Monotone Condition

Inspired by [14], we rely on a regularized formulation to compute the Wasserstein barycenter. However, (6) cannot provide precise approximations in high dimensions [27]. To address this issue, we enforce c -cyclical monotone condition via a regularization.

Given a function $c : \mathcal{X} \times \mathcal{Y} \rightarrow \mathbb{R} \cup +\infty$, a set $\Gamma \subseteq \mathcal{X} \times \mathcal{Y}$ is said *c-cyclical monotone*, if for any permutation σ , any $k \in \mathbb{N}$ and any finite pairs $(x^1, y^1), \dots, (x^k, y^k) \in \Gamma$, one have

$$\sum_{i=1}^k c(x^i, y^i) \leq \sum_{i=1}^k c(x^i, y^{\sigma(i)}) \quad (7)$$

For a finite set Γ , c -cyclical monotonicity means the points of origin x^i and destination y^i related by (x^i, y^i) have been paired so as to minimize the total transportation cost $\sum_{\Gamma} c(x, y)$. Otherwise it would be more efficient to move mass from all x^i to y^i .

Importantly, c -cyclical monotonicity is a necessary condition for optimality in OT [30].

Theorem 1 (γ has a c -cyclical monotone support). *If γ is an optimal transport plan for the Wasserstein distance (i.e., it minimizes problem (1)) and c is continuous, then the support of γ , i.e., Γ is a c -cyclical monotone set.*

This theorem can be proved by contradiction. The detailed discussion can be found in [31].

In order to enforce c -cyclical monotonicity, we define

$$I(x, y) = \sup_{k \geq 2} \sum_{i=1}^k c(x^i, y^i) - \sum_{i=1}^k c(x^i, y^{\sigma(i)}) \quad (8)$$

Then $I : \mathcal{X} \times \mathcal{Y} \rightarrow [0, \infty]$. For all $(x, y) \in \Gamma$, $I = 0$ since Γ is c -cyclically monotone.

Combing the constraint of dual formulation $\phi(x^i) + \psi(y^i) \leq c(x^i, y^i)$, we want to maximize $\sum_{i=1}^k \phi(x^i) + \psi(y^i) - \sum_{i=1}^k c(x^i, y^{\sigma(i)})$. The supremum value of this difference is zero when $(x^i, y^i) \in \Gamma$. But outside Γ , we expect the supremum value is greater than zero. Hence we consider an additional convex regularization:

$$F\left(\sum_{i=1}^k c(x^i, y^{\sigma(i)}) - (\phi(x^i) + \psi(y^i))\right), \quad (9)$$

where F refers to either entropy or L^2 -norm regularization defined in (4).

Plugging (9) into the regularized Wasserstein barycenter problem (6), we obtain the following objective:

$$\inf_{\nu} \sup_{\phi, \psi} \sum_{i=1}^N \alpha_i \left[\int_{\mathcal{X}} \phi_i(x_i) \mu_i(x_i) dx_i + \int_{\mathcal{X}} \int_{\mathcal{Y}} R(\phi_i(x_i), \psi_i(y)) \mu_i(x_i) \nu(y) dx_i dy \right] \quad (10)$$

where

$$\begin{aligned} R(\phi_i(x_i), \psi_i(y)) &\triangleq F\left(\sum_{l=1}^k c(x_i^l, y^{\sigma(l)}) - \phi_i(x_i^l) - \psi_i(y^{\sigma(l)}) + \sum_{j=1}^N \alpha_j \psi_j(y^{\sigma(l)})\right) \\ &\quad + F(\phi_i(x_i) + \psi_i(y) - \sum_{j=1}^N \alpha_j \psi_j(y) - c(x_i, y)) \end{aligned} \quad (11)$$

Note that we replace each ψ_i with $\psi_i - \sum_{j=1}^N \alpha_j \psi_j$ to obtain an unconstrained version.

For a fixed barycenter ν , the above objective is concave with respect to μ_i and ν which can be maximized through stochastic gradient methods, where dual variables ϕ_i and ψ_i are parameterized as deep neural networks for their ability to approximate general functions.

3.2 Introducing a Variational Distribution

In the context of estimating barycenters of continuous distributions, we propose to represent the barycenter using a variational distribution $\nu'(\cdot|\lambda)$. If we know the input distributions are in the same family, e.g., Gaussian, we can set the variational distribution ν' to be a Gaussian with unknown mean and covariance. Otherwise we consider $\nu' = \prod_{i=1}^N \nu'_i(\cdot|\lambda_i)$, where the type of ν'_i coincides with each input distribution μ_i . In the case where a fix set of samples is provided and no information about the barycenter is known beforehand, we can assume that the variational distribution is a Gaussian mixture, which has the ability to approximate any functions [32].

Having specified a variational distribution $\nu'(y|\lambda)$, we transform the barycenter estimation problem into an optimization problem that minimizes the following objective to determine the values of variational parameters λ :

$$\sum_{i=1}^N \alpha_i W_p^p(\mu_i(x_i), \nu'(y|\lambda)) \quad (12)$$

Then the regularized version is to re-write (10) as follows:

$$\mathcal{L} \triangleq \sum_{i=1}^N \alpha_i \left[\int_{\mathcal{X}} \phi_i(x_i) \mu_i(x_i) dx_i + \int_{\mathcal{X}} \int_{\mathcal{Y}} R(\phi_i(x_i), \psi_i(y)) \mu_i(x_i) \nu'(y|\lambda) dx_i dy \right] \quad (13)$$

Thus we transform the continuous Wasserstein barycenter objective into a tractable form with respect to neural networks and variational parameters. We can optimize the objective \mathcal{L} through stochastic gradient methods.

The noisy gradients of \mathcal{L} To optimize the objective \mathcal{L} with gradient-based methods, we need to develop an unbiased estimator of its gradients which can be computed using Monte Carlo samples. To do this, we derive gradients of \mathcal{L} with respect to λ as an expectation form:

$$\begin{aligned} \nabla_{\lambda} \mathcal{L} &= \nabla_{\lambda} \sum_{i=1}^N \alpha_i \int_{\mathcal{X}} \int_{\mathcal{Y}} R(\phi_i(x_i), \psi_i(y)) \mu_i(x_i) \nu'(y|\lambda) dx_i dy \\ &= \sum_{i=1}^N \alpha_i \int_{\mathcal{X}} \int_{\mathcal{Y}} \nabla_{\lambda} R(\phi_i(x_i), \psi_i(y)) \mu_i(x_i) \nu'(y|\lambda) dx_i dy \\ &= \sum_{i=1}^N \alpha_i \mathbb{E}_{\mu_i \nu'} [\nabla_{\lambda} \log \nu'(y|\lambda) R(\phi_i(x_i), \psi_i(y))] \end{aligned} \quad (14)$$

where $\nabla_{\lambda} \log \nu'(y|\lambda)$ is called the score function [33], and it can be calculated using automatic differentiation tools [34]. Note that $\nabla_{\lambda} [\nu'(y|\lambda)] = \nabla_{\lambda} [\log \nu'(y|\lambda)] \nu'(y|\lambda)$.

With this equation in hand, we can directly compute the gradient using Monte Carlo samples

drawn from $\mu(x)\nu'(y|\lambda)$:

$$\begin{aligned}\nabla_\lambda \mathcal{L} &\approx \frac{1}{S} \sum_{i=1}^N \sum_{s=1}^S \alpha_i \nabla_\lambda \log \nu'(y^{(s)}|\lambda) R(\phi_i(x_i^{(s)}), \psi_i(y^{(s)})) \\ x_i^{(s)} &\sim \mu_i(x_i), y^{(s)} \sim \nu'(y|\lambda)\end{aligned}\tag{15}$$

where S is the number of Monte Carlo samples. Then, at each iteration t , the parameter of interest λ can be updated as follows:

$$\lambda_t \leftarrow \lambda_{t-1} - \rho_t \nabla_\lambda \mathcal{L},\tag{16}$$

where ρ_t is the learning rate.

Note that the optimization over ν is not convex. However it guarantees to converge to a local optimum, if the learning rate satisfies the Robbins-Monro condition [35]:

$$\sum_{t=1}^{\infty} \rho_t = \infty, \quad \sum_{t=1}^{\infty} \rho_t^2 < \infty$$

Variance reduction The noisy gradients formed by using Monte Carlo samples often can be too large to be useful. In practice, the high variance would lead to slow convergence and even worse performance [36, 37].

To alleviate this, we use the control variate to reduce variance [36, 38], which is a family of functions with equivalent expectation. The basic idea is to replace the target function with another function which has the same expectation but smaller variance. For example, when we compute $\mathbb{E}[f]$ with Monte Carlo samples, we use the empirical average of \hat{f} where \hat{f} is chosen so $\mathbb{E}[f] = \mathbb{E}[\hat{f}]$ and $\text{Var}[f] > \text{Var}[\hat{f}]$. Next we describe how to reduce the variance via easy-to-implement control variates.

Define \hat{f} to be

$$\hat{f}(z) \triangleq f(z) - a(h(z) - \mathbb{E}[h(z)]),$$

where $h(z)$ is a function with a finite first moment, and a is a scalar. Note that $\mathbb{E}[f] = \mathbb{E}[\hat{f}]$ as required. The variance of \hat{f} is:

$$\text{Var}(\hat{f}) = \text{Var}(f) + a^2 \text{Var}(h) - 2a \text{Cov}(f, h)$$

This equation implies that a good control variate \hat{f} with smaller variance will have high covariance with the function f . Given a function h , taking the derivative of $\text{Var}(\hat{f})$ with respect to a and setting it equal to zero, one can get the optimal scaling,

$$a^* = \text{Cov}(f, h) / \text{Var}(h),$$

which can be estimated with the ratio of empirical covariance and variance using Monte Carlo samples.

Inspired by this, in our method we choose h to be the score function of the variational distribution, i.e., $\nabla_\lambda \log \nu'(y|\lambda)$ which always has expectation zero, and re-compute the gradient of \mathcal{L} with respect to λ using a new Monte Carlo method:

$$\begin{aligned}\nabla_\lambda \mathcal{L} &\approx \frac{1}{S} \sum_{i=1}^N \sum_{s=1}^S \alpha_i \nabla_\lambda \log \nu'(y^{(s)}|\lambda) (R(\phi_i(x_i^{(s)}), \psi_i(y^{(s)})) - a^*) \\ x_i^{(s)} &\sim \mu_i(x_i), y^{(s)} \sim \nu'(y|\lambda)\end{aligned}\tag{17}$$

Algorithm 1 Optimization of VWB

```
1: Input: Continuous distributions  $\{\mu_i\}_{i=1}^N$  with weight  $\alpha_i$ ; cost function  $c$ ; batch size  $S$ ; regularization  $R$ ; learning rate  $\rho$ ; the network gradient update function BackWard.
2: While not converged do
3:    $\forall i \in \{1, \dots, N\}$ : sample  $x_i$  from  $\mu_i$ 
4:   sample  $y$  from  $\nu'(y|\lambda)$  and obtain a permutation  $y^\sigma$ 
5:    $\bar{\psi} \leftarrow \sum_{j=1}^N \alpha_i \psi_j(y)$ ;  $\hat{\psi} \leftarrow \sum_{j=1}^N \alpha_i \psi_j(y^\sigma)$ 
6:   For  $i = 1$  to  $N$  do
7:      $R_i^1 \leftarrow F(\sum_{l=1}^S c(x_i^l, y^{\sigma(l)}) - \phi_i(x_i^l) - \psi_i(y^{\sigma(l)}) + \hat{\psi})$ 
8:      $R_i^2 \leftarrow F(\phi_i(x_i) + \psi_i(y) - \bar{\psi} - c(x_i, y))$ 
9:      $R_i \leftarrow R_i^1 + R_i^2$ 
10:  End For
11:   $F \leftarrow \sum_{i=1}^N \alpha_i (\phi_i(x_i) + R_i)$ 
12:  For  $i = 1$  to  $N$  do in parallel
13:    BackWard( $F, \phi_i$ ); BackWard( $F, \psi_i$ )
14:  End For
15:   $f \leftarrow \sum_{i=1}^N \alpha_i \nabla_\lambda \log \nu'(y|\lambda) R_i$ 
16:   $h \leftarrow \nabla_\lambda \log \nu'(y|\lambda)$ 
17:   $a^* \leftarrow \text{Cov}(f, h) / \text{Var}(h)$ 
18:  update  $\lambda \leftarrow \lambda - \rho(f - a^* h)$ 
19: End While
20: Output: The continuous Wasserstein barycenter  $\nu'$  of  $\{\mu_i\}_{i=1}^N$ .
```

Full algorithm We summarize the full algorithm of VWB in *Algorithm 1*.

Discussion In practice, we replace $\sum_{i=1}^k c(x^i, y^{\sigma(i)})$ with $\sum_{i=1}^k c(x^i, y^{i+1})$ in the regularization (with the obvious convention $y^{k+1} = y^1$), and set k equal to the number of Monte Carlo samples as indicated in *Algorithm 1*. It is enough to check c -cyclical monotonicity.

Computation complexity For our method, as well as the methods proposed in [14, 27], computing the Wasserstein barycenter of N input distributions includes repeated computation of N Wasserstein distances having a $O(NSP)$ complexity per iteration where P is the size of the networks. Afterwards, the methods in [14, 27] recover the barycenter by an additional calculation, which is not an easy task with square level complexity at least. However, our method is end-to-end and can easily be parallelized. Since dual variable pair $(\phi_i, \psi_i), \dots, (\phi_N, \psi_N)$ are uncoupled. After generating samples from variable ν' , N dual variable pairs (ϕ_i, ψ_i) can be computed in a fully parallel manner on N worker threads without information pass between threads. In particular, the master thread iteratively provides samples and updates ν' .

3.3 Theoretical Results

In this section, we discuss the theoretical guarantee for the convergence of our method.

The work [15] shows if at least one of the distributions μ_i is absolutely continuous, then the Wasserstein barycenter ν is unique. Moreover, ν is also absolutely continuous. This analysis ensures the existence and uniqueness of the Wasserstein barycenter for continuous distributions.

Theorem 2 (Convergence). *Let μ_1, \dots, μ_N be continuous distributions with respect to the Lebesgue measure. Assume the cost c is continuous on $\mathcal{X} \times \mathcal{Y}$. If $\{\phi_i, \psi_i\}_{i=1}^N$ are the optimal dual potentials in (10), then each $\{\phi_i, \psi_i\}$ is a solution to the regularized dual formulation (3). Let ν^ε the solution of regularized Wasserstein barycenter problem (10), and let ε converging to 0 sufficiently fast. Then, ν^ε converges weakly to the solution ν of the Wasserstein barycenter problem (5).*

We include a proof of Theorem 2 in the supplementary document.

4 Experiments

In this section, we demonstrate the effectiveness of our method VWB on both synthetic and real data.

4.1 Experimental Setup

Our aim is to examine whether VWB can accurately approximate the continuous barycenter. To this end, we compute the Wasserstein barycenter of multivariate Gaussian distributions, with the squared Euclidean distance as the cost function, i.e., $c(x, y) = \|x - y\|_2^2$, $x, y \in \mathbb{R}^D$. In all experiments, we use equal weights for input distributions, i.e., $\alpha_i = \frac{1}{N}$ for all $i = 1, \dots, N$. Note that the proposed method is not limited to Euclidean distance and equal weights, which can be applied to a more general setting.

We compare VWB against the following state of the art methods: (i) continuous regularized Wasserstein barycenter (CRWB) ¹ [14]; (ii) continuous Wasserstein barycenter without minimax optimization (CWB) ² [27]; (iii) scalable computations of Wasserstein barycenter via input convex neural networks (SCWB) ³ [26]. These methods recover barycenter through gradient-based method. In CRWB, we consider L^2 -norm regularization since it performs better than entropy regularization.

In our method, we use the Adam method to adjust learning rate, where parameters $\beta_1=0.9$, $\beta_2=0.999$ and $\alpha=0.001$. The dual variables $\{\phi_i, \psi_i\}_{i=1}^N$ are parameterized as neural networks with two fully-connected hidden layers ($D \rightarrow 128 \rightarrow 256 \rightarrow D$) using ReLU activations. The choice of the number of samples and iterations depends on the examples. ε in L^2 -norm regularization is set to 10^{-4} or 10^{-5} , and ε in entropy regularization is set to 10^{-1} . Besides, we report the average results of 5 independent runs.

4.2 Learning the Wasserstein Barycenter in 2D

Figure 2 shows the qualitative performance of our methods on 2D examples. Each example is represented in a row. The first column is the input distributions, and the second column is the approximated barycenter using our method VWB with L^2 -norm regularization. In the first example, we set the variational distribution ν' to be a uniform distribution times a circular distribution. In the second example, we set ν' to be a Gaussian mixture. We can observed that VWB L^2 -norm regularization learns the barycenter qualitatively well.

¹<https://github.com/lingxiaoli94/CWB>

²<https://github.com/iamalexkorotin/Wasserstein2Barycenters>

³<https://github.com/sbyebs/Scalable-Wasserstein-Barycenter>

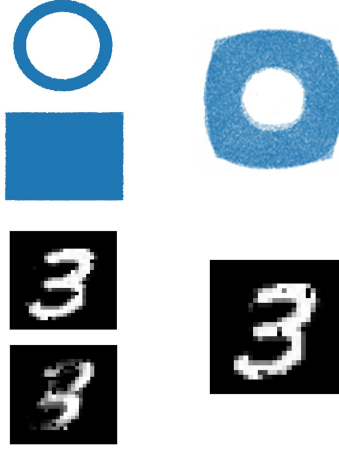


Figure 2: Qualitative results of VWB L^2 -norm regularization in 2D setting. The first column is the input distributions, and the second is the barycenter learned by our method.

4.3 Evaluation on Multivariate Gaussians

We compute the Wasserstein barycenters of N multivariate Gaussians $\mathcal{N}(m_i, \Sigma_i)$ in dimension D with zero mean. The covariance matrix Σ_i is generated by sampling a matrix A with uniform entries in $[-2, 2]$ and then compute AA^T as Σ_i . When the input distributions are multivariate Gaussians, the Wasserstein barycenter is always a Gaussian $\mathcal{N}(m_*, \Sigma_*)$, where $m_* = \sum_{i=1}^N \alpha_i m_i$ and $\Sigma_* = \sum_{i=1}^N \alpha_i (\Sigma_*^{\frac{1}{2}} \Sigma_i \Sigma_*^{\frac{1}{2}})^{\frac{1}{2}}$ computed through an efficient fixed-point algorithm [39].

To evaluate the performance of these methods, we use the Bures-Wasserstein UVP measuring whether the approximation of the Wasserstein barycenter, denoted by ν with mean m_ν and covariance Σ_ν , approach the true one $\tilde{\nu}$ mean $m_{\tilde{\nu}}$ and covariance $\Sigma_{\tilde{\nu}}$ [27]:

$$\text{BW}_2^2 - \text{UVP}(\nu, \tilde{\nu}) \triangleq 100 \frac{\text{BW}_2^2(\nu, \tilde{\nu})}{\frac{1}{2} \text{Var}(\tilde{\nu})} \%, \quad (18)$$

where $\text{BW}_2^2(\nu, \tilde{\nu})$ equals

$$\frac{1}{2} \|m_\nu - m_{\tilde{\nu}}\|^2 + \frac{1}{2} \text{Tr} \left(\Sigma_\nu + \Sigma_{\tilde{\nu}} - 2(\Sigma_\nu^{1/2} \Sigma_{\tilde{\nu}} \Sigma_\nu^{1/2})^{1/2} \right).$$

Here $\text{Tr}(\cdot)$ denotes the trace of a matrix. When $\text{BW}_2^2 - \text{UVP} \approx 0\%$, ν is a good approximation of $\tilde{\nu}$. In the case of $\text{BW}_2^2 - \text{UVP} \geq 100\%$, the approximation ν is undesirable.

The results of 3 randomly generated multivariate Gaussians in varying dimensions D are shown in Table 2. In our method VWB, we consider L^2 -norm regularization as well as in [14]. We can find the estimation errors of VWB with L^2 -norm regularization are lower than those of other methods in all cases. These results imply our method can make good approximations of the Wasserstein barycenters. The estimation error of VWB with L^2 -norm regularization shows a slow rate of growth with respect to dimension compared with other methods CRWB and SCWB. In particular, CRWB does not scale well to higher dimensions.

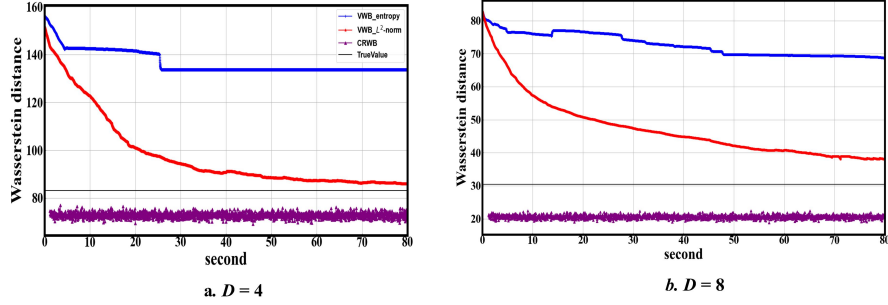


Figure 3: Convergence curves of CRWB and VWB with L^2 -norm and entropy regularization at $D=4$ and 8.

D	VWB with L^2 -norm (Ours)	CRWB [14]	CWB [27]	SCWB [26]
2	0.01	0.2	0.06	0.02
4	0.04	1.2	0.06	0.12
8	0.09	6.41	0.17	0.11
16	0.23	17.83	0.20	0.11
32	0.20	54.12	0.21	0.40
64	0.23	>100	0.25	15.67
128	1.39	>100	1.42	>100

Table 2: Numerical results of the $BW_2^2 - \text{UVP}$ error with dimension for estimating barycenters of Gaussian distributions. Smaller is better.

Convergence We show the convergence curves of VWB with L^2 -norm and entropy regularization and closely related method CRWB at $D=4$ and 8 within 80 seconds in Figure 3. We can observe that VWB with L^2 -norm converges faster to the true value in both settings than other two methods. In particular, we find that the convergence rate of CRWB fluctuates very flatly. The reason is that CRWB fixes a prior as the approximation of the barycenter at the beginning and only optimizes the dual variables using samples from the prior. This result demonstrates that the choice of the prior directly influences the performance of CRWB. On the other hand, VWB with entropy regularization is less stable since there is an exponential term causing overflow.

4.4 Evaluation on Real Data

We now evaluate VWB in real-world applications. We apply the Wasserstein barycenter to aggregate posterior distributions of subsets in a large data set to approximate the true posterior of the full data. Following [14], we use Poisson regression for the task of predicting the hourly number of bike

Method	$BW_2^2 - UVP$
VWB with L^2 -norm (Ours)	0.09
CRWB [14]	0.24
CWB [27]	0.12
SCWB [26]	0.12

Table 3: Empirical results on subset posterior aggregation. The $BW_2^2 - UVP$ is computed for comparison by VWB with L^2 -norm regularization, CRWB, CWB and SCWB.

rentals using features such as the day of the week and weather conditions ⁴, where the number of regression coefficients is set to 8. Here, we estimate the posterior distribution on the regression coefficients. We firstly randomly split the full data into 5 subsets with equal-size and compute the posterior distributions of subsets with 10^5 samples as the input distributions. Then we compute the Wasserstein barycenter of these subset posterior distributions as the approximation of posterior of the full data by using VWB with L^2 -norm regularization, CRWB, CWB and SCWB. To evaluate the performance of these methods, we compute the Bures-Wasserstein UVP between the approximated barycenter and the true posterior distribution of the full data.

The results are shown in Table 3. All methods approach the true Wasserstein barycenter well since the value of $BW_2^2 - UVP < 1\%$. The performance of VWB with L^2 -norm regularization is competitive with CWB and SCWB, and better than CRWB. This further indicates that VWB is an effective alternative to compute continuous Wasserstein barycenters.

5 Conclusion

We develop a novel VWB method to compute the Wasserstein barycenters of continuous distributions. We introduce a variational distribution to represent the continuous barycenter and construct a tractable dual regularized objective with c -cyclical monotonicity to make good approximations. The objective can be solved by alternative stochastic optimization only requiring samples access to the input distributions, where the parameters of the variational distribution can be optimized to find the closest one as the approximation of true barycenter. We prove a theoretical analysis on convergence of our method. Empirical studies on both real and synthetic data demonstrate the effectiveness of VWB.

Acknowledgement

We would like to acknowledge support for this project from China Postdoctoral Science Foundation [No.2019M661210], National Natural Science Foundation of China (NSFC) [No.62006094].

References

- [1] Sanvesh Srivastava, Volkan Cevher, Quoc Dinh, and David Dunson. Wasp: Scalable bayes via barycenters of subset posteriors. In *Artificial Intelligence and Statistics*, pages 912–920, 2015.

⁴<http://archive.ics.uci.edu/ml/datasets/Bike+Sharing+Dataset>

- [2] Alexandre Gramfort, Gabriel Peyré, and Marco Cuturi. Fast optimal transport averaging of neuroimaging data. In *International Conference on Information Processing in Medical Imaging*, pages 261–272, 2015.
- [3] Julien Rabin, Gabriel Peyré, Julie Delon, and Marc Bernot. Wasserstein barycenter and its application to texture mixing. In *International Conference on Scale Space and Variational Methods in Computer Vision*, pages 435–446, 2011.
- [4] Jianbo Ye, Panruo Wu, James Z Wang, and Jia Li. Fast discrete distribution clustering using wasserstein barycenter with sparse support. *IEEE Transactions on Signal Processing*, 65(9):2317–2332, 2017.
- [5] Nhat Ho, Viet Huynh, Dinh Phung, and Michael Jordan. Probabilistic multilevel clustering via composite transportation distance. In *International Conference on Artificial Intelligence and Statistics*, pages 3149–3157, 2019.
- [6] Gaspard Monge. Mémoire sur la théorie des déblais et des remblais. *Histoire de l’Académie Royale des Sciences de Paris*, 1781.
- [7] Leonid Kantorovitch. On the transfer of masses (in russian). *Doklady Akademii Nauk*, 37(2):227–229, 1942.
- [8] Cédric Villani. *Topics in optimal transportation*. Number 58. American Mathematical Society, 2003.
- [9] Cédric Villani. *Optimal transport: old and new*, volume 338. Springer Science & Business Media, 2008.
- [10] Nicolas Bonneel, Julien Rabin, Gabriel Peyré, and Hanspeter Pfister. Sliced and radon wasserstein barycenters of measures. *Journal of Mathematical Imaging and Vision*, 51(1):22–45, 2015.
- [11] Nicolas Bonneel, Gabriel Peyré, and Marco Cuturi. Wasserstein barycentric coordinates: histogram regression using optimal transport. *ACM Trans. Graph.*, 35(4):71–1, 2016.
- [12] Pierre Dognin, Igor Melnyk, Youssef Mroueh, Jerret Ross, Cicero Dos Santos, and Tom Sercu. Wasserstein barycenter model ensembling. *arXiv preprint arXiv:1902.04999*, 2019.
- [13] Gabriel Peyré, Marco Cuturi, et al. Computational optimal transport. *Foundations and Trends® in Machine Learning*, 11(5-6):355–607, 2019.
- [14] Lingxiao Li, Aude Genevay, Mikhail Yurochkin, and Justin M Solomon. Continuous regularized wasserstein barycenters. In *Advances in Neural Information Processing Systems*, 2020.
- [15] Martial Agueh and Guillaume Carlier. Barycenters in the wasserstein space. *SIAM Journal on Mathematical Analysis*, 43(2):904–924, 2011.
- [16] Ethan Anderes, Steffen Borgwardt, and Jacob Miller. Discrete wasserstein barycenters: Optimal transport for discrete data. *Mathematical Methods of Operations Research*, 84(2):389–409, 2016.
- [17] Marco Cuturi and Gabriel Peyré. Semidual regularized optimal transport. *SIAM Review*, 60(4):941–965, 2018.

- [18] Lei Yang, Jia Li, Defeng Sun, and Kim-Chuan Toh. A fast globally linearly convergent algorithm for the computation of wasserstein barycenters. *arXiv preprint arXiv:1809.04249*, 2018.
- [19] Dongdong Ge, Haoyue Wang, Zikai Xiong, and Yinyu Ye. Interior-point methods strike back: solving the wasserstein barycenter problem. In *Advances in Neural Information Processing Systems*, pages 6894–6905, 2019.
- [20] Marco Cuturi and Arnaud Doucet. Fast computation of wasserstein barycenters. In *International Conference on Machine Learning*, pages 685–693, 2014.
- [21] Jean-David Benamou, Guillaume Carlier, Marco Cuturi, Luca Nenna, and Gabriel Peyré. Iterative bregman projections for regularized transportation problems. *SIAM Journal on Scientific Computing*, 37(2):A1111–A1138, 2015.
- [22] Marco Cuturi and Gabriel Peyré. A smoothed dual approach for variational wasserstein problems. *SIAM Journal on Imaging Sciences*, 9(1):320–343, 2016.
- [23] Matthew Staib, Sebastian Clatici, Justin M Solomon, and Stefanie Jegelka. Parallel streaming wasserstein barycenters. In *Advances in Neural Information Processing Systems*, pages 2647–2658, 2017.
- [24] Sebastian Clatici, Edward Chien, and Justin Solomon. Stochastic wasserstein barycenters. In *International Conference on Machine Learning*, pages 999–1008, 2018.
- [25] Pavel Dvurechenskii, Darina Dvinskikh, Alexander Gasnikov, Cesar Uribe, and Angelia Nedich. Decentralize and randomize: Faster algorithm for wasserstein barycenters. In *Advances in Neural Information Processing Systems*, pages 10760–10770, 2018.
- [26] Jiaojiao Fan, Amirhossein Taghvaei, and Yongxin Chen. Scalable computations of wasserstein barycenter via input convex neural networks. *arXiv preprint arXiv:2007.04462*, 2021.
- [27] Alexander Korotin, Lingxiao Li, Justin Solomon, and Evgeny Burnaev. Continuous wasserstein-2 barycenter estimation without minimax optimization. *International Conference on Learning Representations*, 2021.
- [28] Samuel Cohen, Michael Arbel, and Marc Peter Deisenroth. Estimating barycenters of measures in high dimensions. *arXiv preprint arXiv:2007.07105*, 2020.
- [29] Marco Cuturi. Sinkhorn distances: Lightspeed computation of optimal transport. In *Neural Information Processing Systems*, pages 2292–2300, 2013.
- [30] Wilfrid Gangbo and Robert J McCann. The geometry of optimal transportation. *Acta Mathematica*, 177(2):113–161, 1996.
- [31] Aldo Pratelli. On the sufficiency of c-cyclical monotonicity for optimality of transport plans. *Mathematische Zeitschrift*, 258(3):677–690, 2008.
- [32] Yuichiro Anzai. *Pattern recognition and machine learning*. Elsevier, 2012.
- [33] David Roxbee Cox and David Victor Hinkley. *Theoretical statistics*. CRC Press, 1979.
- [34] Stan Development Team. Stan: A c++ library for probability and sampling, version 2.8.0, 2015.

- [35] Herbert Robbins and Sutton Monro. A stochastic approximation method. *The Annals of Mathematical Statistics*, pages 400–407, 1951.
- [36] John William Paisley, David M. Blei, and Michael I. Jordan. Variational Bayesian inference with stochastic search. In *International Conference on Machine Learning*, pages 1367–1374, 2012.
- [37] Ximing Li, Changchun Li, Jinjin Chi, and Jihong Ouyang. Variance reduction in black-box variational inference by adaptive importance sampling. In *International Joint Conferences on Artificial Intelligence*, pages 2404–2410, 2018.
- [38] Sheldon M Ross. *Simulation*. Elsevier, 2002.
- [39] Pedro C Álvarez-Esteban, E Del Barrio, JA Cuesta-Albertos, and C Matrán. A fixed-point approach to barycenters in wasserstein space. *Journal of Mathematical Analysis and Applications*, 441(2):744–762, 2016.